Digest Journal of Nanomaterials and Biostructures Vol. 19, No. 3, July -September 2024, p. 1173 - 1186

Incorporation of B and La oxides into bioactive glass: in vitro studies for bone regeneration applications

R. Badraddin[a], E. Koç[a], A. N. Saud[a,b,*]
[a]*Department of Biomedical Engineering, Faculty of Engineering, Karabük University, Turkey*
[b]*Biomedical Engineering, Al-Mustaqbal University College, Babylon, Iraq*

Bone tissue engineering seeks to regenerate damaged tissues using biocompatible scaffolds that mimic bone minerals. This study focuses on scaffolds based 45S5 bioactive glass (45% SiO_2, 24.5% Na_2O, 6% P_2O_5, 24.5% CaO) doped with boron and lanthanum oxides. These scaffolds, produced via conventional melting, form a hydroxyapatite layer, promoting strong bone integration. Result of DTA, XRD, FTIR, SEM, and EDS, showed doping led to crystalline phase identification, silicate network confirmation, and detection of calcium phosphorus deposits. Doping also increased pH, degradation kinetics, and antibacterial activity. These findings suggest that boron and lanthanum-doped 45S5 scaffolds have potential in bone regeneration applications.

(Received May 28, 2024; Accepted August 4, 2024)

Keywords: Bioactive glass, Doping, Bioactivity, Hydroxyapatite, Mechanical properties

1. Introduction

The skeletal system is the most important part of our body. It gives our body its shape, keeps it upright, and protects our internal organs from external influences. Injuries that happen in this system, Minor injuries to the bone structure are healed in a short time through the mechanism of the skeletal system but large injuries don't heal quickly in such cases, so the use of implant material is necessary [1]. The biomaterials as implant materials that replace bone tissue in the body have appropriate mechanical properties and the body accepts them, Biomaterials should have appropriate mechanical properties, be non-toxic, have high biocompatibility, must be resistant to corrosion in body fluids, and must have features such as being resistant to the loads that occur in normal physical movements [2]. Biomaterials can generally be categorized into four main classes based on their composition: metals, ceramics, polymers, and composites. Ceramic biomaterials developed for use in medical applications such as repairing, reconstructing, or replacing tissues are referred to as ''bioceramic'' [3]. Since bioactive glasses are biocompatible, bioactive, osteoconductive, and bone-productive, they have garnered the most attention in relation to bone regeneration [4]. Since the bone is brittle and has a low mineral density, these bioactive materials are used as implants to promote healing, particularly in situations where metallic reinforcement is not appropriate [5]. Bioactive glasses can be made using two different methods: the sol-gel method, which involves low temperatures, or the traditional melting method, which involves high temperatures [6].

Bioactive glasses and bioactive glass ceramics are materials with a high density, low mechanical strength, brittleness, inflexibility, and difficulty in processing. Despite these drawbacks, these materials are crucial for medical applications due to their exceptional biocompatibility and corrosion resistance. When bioactive materials meet physiological fluid, they generally form a surface layer resembling apatite [7]. Bioglasses are silicate glasses with phosphate, calcium, and sodium in them. Conversely, bioactive glass-ceramics are polycrystalline, Bioglasses used in specific areas of medicine. In dentistry (upper jaw and face treatment, dental socket treatment, periodontal area wear), as well as middle ear bone treatment, bioactive glass-ceramic is used when treating heavier-loading areas like the pelvis and waist bone [8]. Several bioactive glasses are primarily composed of SiO_2, Na_2O, CaO, and P_2O_5. 45S5 is the first and best composition of bioactive

* Corresponding author: Amir.saud92@gmail.com
https://doi.org/10.15251/DJNB.2024.193.1173

glass. Each code used to identify a classified compound is linked to a specific compound type. Formula code 45S5 serves as the basis for many bioactive silicate glasses that were later produced. Put differently, the weight percentage of SiO_2 is 45% and the CaO/P_2O_5 ratio is 5:1 [9]. The concentration of SiO_2 in bioactive glasses determines their bioactivity. As a result, bioactive glass has three fundamental compositional characteristics that give it a very reactive surface. These include less than 60 mol%SiO_2, high Na_2O and CaO contents, high CaO/P_2O_5 ratios, and high CaO and P_2O_5 contents in glasses without partial devitrification [10]. The interface bonding between the implant and tissue is referred to as "bioactive glass" by Hench. The most common characteristic of materials is the formation of a hydroxycarbonate apatite (HCA) layer on the surface, which was initially reported by Hench [11] and subsequently by Davies [12].

Bioactive glasses uniquely possess osteogenic properties that stimulate both the proliferation and differentiation of osteoprogenitor cells. While many biomaterials used over the years for bone regeneration exhibit bioactivity and osteoconductive properties, they often suffer from high solubility and poor mechanical attributes, such as low toughness and fracture resistance. To enhance the therapeutic qualities, mechanical strength, and biochemical behavior of bioactive glasses, ion doping with various elements is a widely recognized approach. The bioactivity of these glasses is heavily influenced by their surface composition and reactivity. Research over the years has explored the effects of several metals and additive ions, particularly those prevalent in human bone, such as magnesium, strontium, fluoride, potassium, and zinc, on the biomechanical and biological behavior of bioactive glasses [13].

Boron (B) plays a crucial role in the health of both humans and animals. Recently, boron-based bioactive glasses (BBGs) have been explored for various biomedical applications, including controllable glass dissolution, angiogenesis, osteogenesis, tissue infiltration support, enhanced coating adhesion, and improved mechanical properties. Additionally, boron aids in regulating protein and collagen release, which is beneficial for wound healing. As a newer addition to the bioactive glass family, BBGs are known for their osteoconductive and biodegradable properties, making them promising candidates for regenerative medicine, tissue engineering, and wound care.[14]. Lanthanum (La), a rare earth element with properties similar to calcium (Ca), is found in bones. Lanthanum carbonate has been proposed as an alternative to calcium-based phosphate binders for treating end-stage renal disease (ESRD). Studies have shown that La-doped bioactive glasses are non-toxic up to 10 mol% and exhibit antibacterial properties. Composites of hydroxyapatite (HA) and La demonstrate enhanced biocompatibility and bioactivity in simulated body fluid (SBF). Research indicates that La ions positively influence the proliferation and osteogenic differentiation of mesenchymal cells. Furthermore, La doping improves the mechanical properties, such as elastic modulus and hardness, of silicate-containing glasses, along with enhancing their thermal stability.[13].

This study aims to enhance the mechanical and biological properties of bioactive glass scaffolds for bone tissue engineering by incorporating boron and lanthanum. The structural and morphological characteristics of the prepared bioactive glasses were examined using differential thermal analysis (DTA), X-ray diffraction (XRD), Fourier transform infrared spectroscopy (FTIR), and scanning electron microscopy (SEM). Additionally, the bioactive glasses were immersed in simulated body fluid (SBF) for specific time intervals to assess their bioactivity, weight loss, pH changes, and biodegradability. In vitro antibacterial tests and compression tests were also conducted on the bioactive glass scaffolds to evaluate their performance.

2. Materials and methods

2.1. Synthesis of bioglass ceramic powder

Using the classical melting method, bioactive glass samples were prepared with the SiO_2-Na_2CO_3-P_2O_5-CaO-xB_2O_3 and La_2O_3 system, four samples with different percentages of boron and lanthanum oxide, as shown in Table (1) For production, the starting mixture was first made from the high-quality raw materials SiO_2, Na_2CO_3, P_2O_5, CaO, B_2O_3, and La_2O_3 from Merck to obtain a more homogeneous mixture. It was crushed in an agate mortar. Then, the powder mixture was melted at 1000 °C in a Protherm PLF-1600 furnace in an alumina crucible, and the melt was kept at this

temperature for 2.5 hours and then poured into pure water. To ensure homogeneity, the obtained granulated glass particles were ground again in an agate mortar and kept in the oven at the same temperature for 2 hours to reduce the viscosity and make the glass easier to cast. The resulting homogeneous glass melts were cast into graphite molds preheated to 300–400 °C to prevent thermal shock.

Table 1. Bioactive glass compositions.

Sample	The weight percentage of each element (wt.%)					
	SiO_2	**Na_2Co_3**	**CaO**	**P_2O_5**	**B_2O_3**	**La_2O_5**
S1	45.0	24.5	24.5	6.0	-	-
S2	43.0	20.5	20.5	6.0	10.0	-
S3	39.0	24.5	24.5	6.0	-	5.0
S4	38.0	20.5	20.5	6.0	10.0	5.0

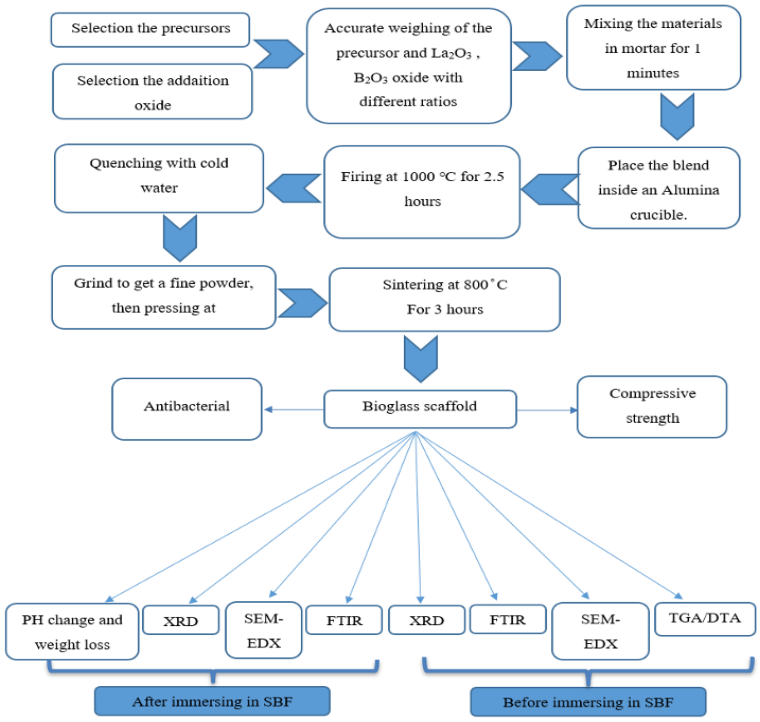

Fig. 1. The experimental program.

2.2. Preparation of bioglass samples

In the experimental setup, cylindrical samples with dimensions (10*22 mm) and (2*5 mm) in diameter and length were produced using a mold and subjected to a compression force of 150 MPa. A 1.5 vol% polyvinyl alcohol (PVA) solution with a molecular weight of 6 kDa (kilo Dalton=1000 dalton) was prepared at a controlled temperature of 60 °C using magnetic agitation. This PVA solution served as a binder when mixed with BG powders and maintained a mass ratio of 0.6:1 between the solution and the powders. The use of a binder is crucial as it increases the plasticity of the powder mixture, reducing the risk of cracking during the compaction process. A temperature of 70°C was maintained for the entire day while the mixture was dried in the oven. The "green" pellets needed to be heated to 800 °C for three hours in an electric oven, with a controlled temperature increase and holding rate of 3 °C per minute. The furnace was allowed to naturally cool after the heating process.

2.3. Characterization

Bioactive glass scaffolds containing boron and lanthanum 45S5, which is composed of 45% SiO_2, 24.5% Na_2O, 6% P_2O_5, 24.5% CaO, and bioactive material, which is composed of 45% SiO_2, 22.5% Na_2O, 6% P_2O_5, 22.5% CaO, and 4% B_2O_3 + La_2O_3 by weight investigated by differential thermal analysis (DTA), X-ray diffraction (XRD), Fourier transform infrared spectroscopy (FTIR), and Glass specimens were subjected to the formation of the hydroxyapatite layer on their surfaces using 30 milliliters of simulated body fluid (SBF). were put inside tubes for centrifuges. These scaffold-containing solutions were then kept for one, seven, and fourteen days in the laboratory at 37 °C in an oven.

To study the biodegradation behavior in vitro, samples were placed in 30 mL of SBF solution and stored in an oven with the temperature set at 37 °C for 1, 7, and 14 days. At the end of the determined periods, the wet weights (W_w) of the scaffolds removed from the SBF solution, their weights after drying (W_d), and their initial weights (W_i) before placing them in artificial body fluid were recorded by weighing the scaffolds. The pH change and weight loss (WL) values were each calculated using an equation [9].

$$Weight\ loss\ \% = \frac{\Delta W}{W_0}$$

The hydroxyapatite layer formed on the scaffold surfaces, its structural morphology after soaking in artificial body fluid, and the porous structure of the materials were all examined under a scanning electron microscope (SEM). Compressive strength tests are often performed for the mechanical properties of bones. Three samples per ratio are tested for consistency under identical conditions. The evaluation was carried out using computer-aided universal testing machines according to the ASTM C-773 standard and was carried out at a constant speed of 0.5 mm/min [15]. The effect of bioactive glass-ceramic samples in bacteria-containing media is carried out in the Kirby-Bauer test using bacteria present in the urine. The basis of this test is the use of an agar tablet that contains bacteria. The samples to be tested as antibiotics are then placed in these tablets for 24 hours. The antibacterial effect of the samples can be recognized by the fact that a circular area forms around the sample. The larger the diameter of the ring, the more effective the sample is as an antibiotic.

3. Results and discussion

DTA was used to analyze the glass transition and crystallization temperatures of five different chemical composition bioactive glass samples that were prepared by the melting method. Glass samples were heated at a rate of 10 °C /min to 900 °C to obtain DTA curves. Weight loss results from the removal of the water and OH groups between 25 °C and 210 °C, 25 °C and 260 °C, and 25 °C and 300 °C, respectively, according to an analysis of the DTA curves Figure (2) of the bioactive glass samples [16]. An endothermic peak indicating the glass transition temperature of the samples and varying between 400 °C and 564 °C and an exothermic peak indicating the crystallization temperature between 724 °C and 800 °C were determined. In general, the glass transition and crystallization temperatures do not change significantly when the amount of lanthanum changes. The crystallization temperatures determined as a result of the analysis show that crystallization occurs in the structure when the sintering temperature of 800 °C required for the production of scaffolds made of bioactive glass is reached [17, 18].

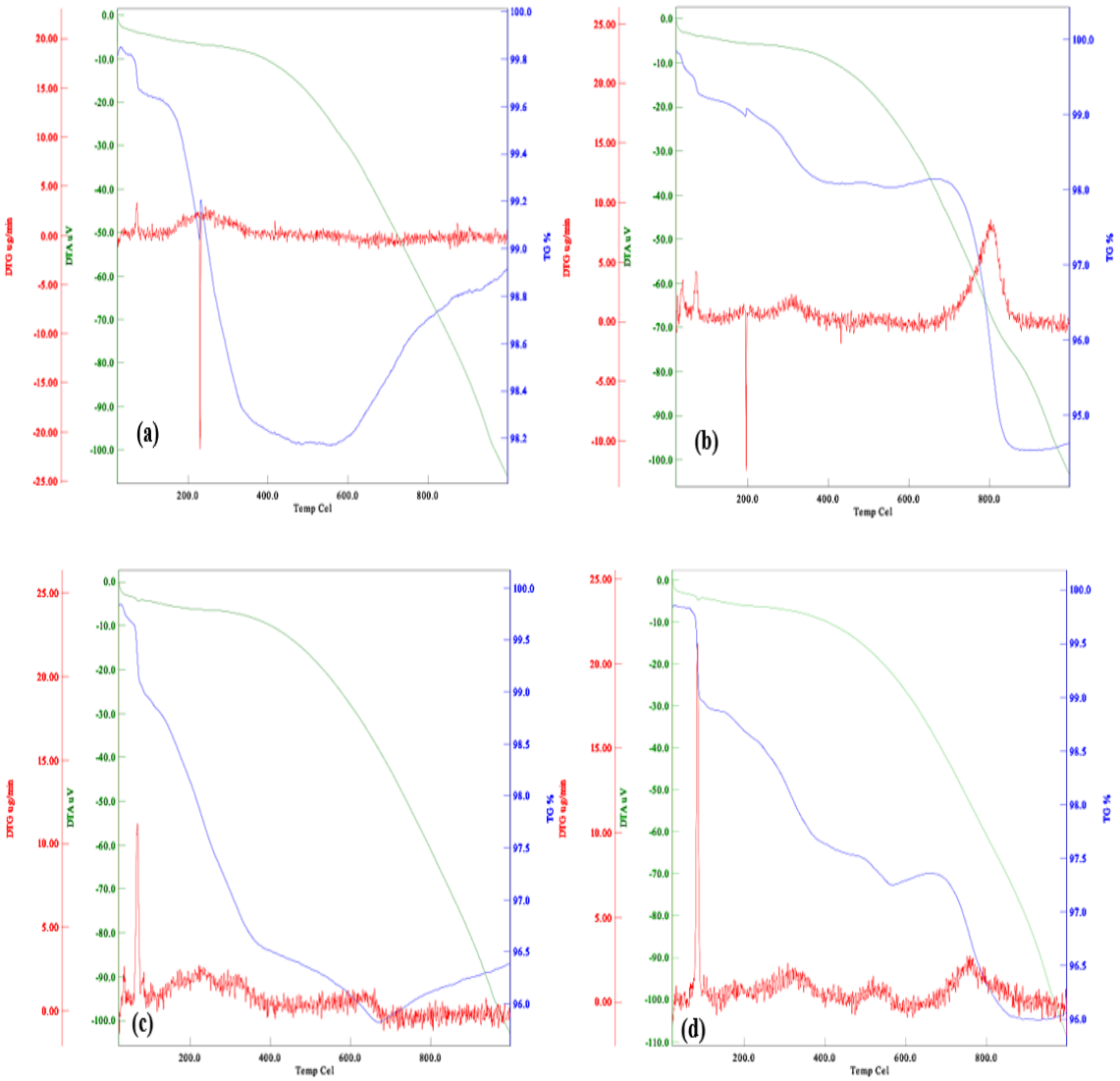

Fig. 2. Thermal analyses of samples a) S1, b) S2, c) S3, and d) S4 From 25 °C to 900 °C.

The XRD diagrams of the bioactive glass samples are shown in Figure 3. The analysis resulted in the crystalline phases sodium calcium silicate $Na_2Ca_2Si_3O_9$ and calcium silicate Ca_2SiO_4. The crystal structure of glass ceramic samples was found to remain unchanged after soaking in synthetic body fluid. Ground and pulverized samples were used for XRD analyses. However, on the surface of samples maintained in artificial body fluid, the amount of HA phase that forms as a thin film is extremely small relative to the overall structure of the sample. Therefore, the thin film XRD method was used to determine the HA layer formed on the surfaces of cylindrical samples. Figure 4 shows the thin film XRD diagram of the bioactive glass samples. As can be observed, HA peaks began to form as early as the first week and their intensity increased during longer waiting periods. This suggests that more HA phase forms on the surfaces of samples kept in artificial body fluid for a long period of time. The width of the XRD pattern was influenced by the size of the crystal and the magnitude of the strain in the lattice. When the amorphous samples were immersed in SBF solution, their initial peak at 32 °C decreased, suggesting the formation of a hydroxyapatite layer on the sample surface and a subsequent decrease in peak intensity [9, 15].

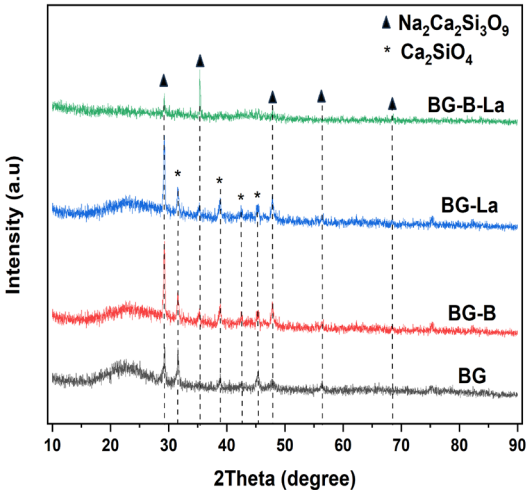

Fig. 3. XRD for the samples before the immersion in SBF.

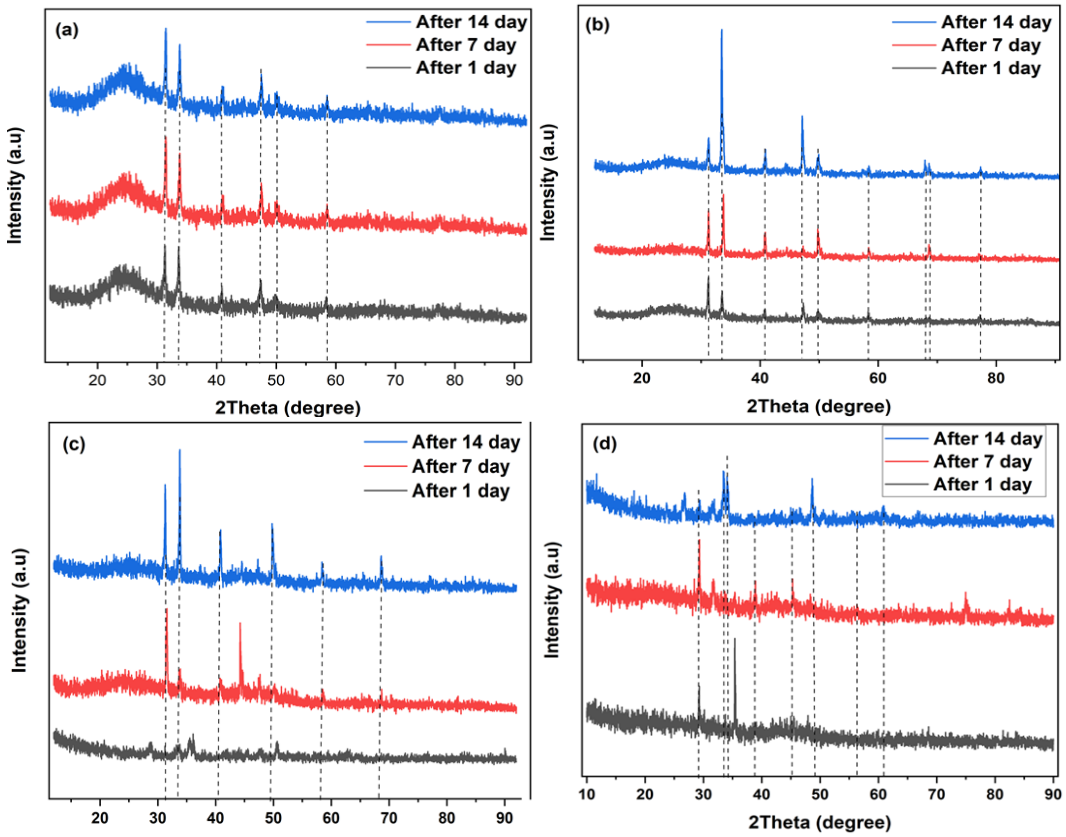

Fig. 4. XRD for samples after SBF immersion. (a) S1, (b) S2, (c) S3, and (d) S4.

The chemical bonds formed in the structures of the bioactive glass and glass-ceramic samples were identified by FTIR analyses. The result shows that as the sample waiting time in the artificial body fluid increases, the formation of HA also increases. It is obvious that the P-O peak intensities are now higher than in the pre-SBF plots. This finding suggests that the longer the samples wait in the artificial body fluid, more HA is formed. In the Na_2O-CaO-SiO_2 system, P-O bonds form at a wavelength of approximately 600 cm^{-1}, with the intensity of the peaks increasing with increasing waiting time in artificial body fluid, according to the literature . Table 2 lists the areas of particular importance.

Table 2. Characterizing bioactive glass surface chemistry transformation through IR analysis of SBF immersion [19].

Wavenumber (Cm^{-1})	Band	Vibrational mode
540-4515	Si-O-Si	Bend
515-530	P-O	Bend crystal
550-560	P-O	Bend amorphous
600-610	P-O	Bend crystal
710-1175	Si-O-Si	Tetrahedral
800-890	C-O	Stretch
860-940	Si-O-Si	Stretch
1100-1250	P=O	Associated
1080-1350	P=O	Stretch

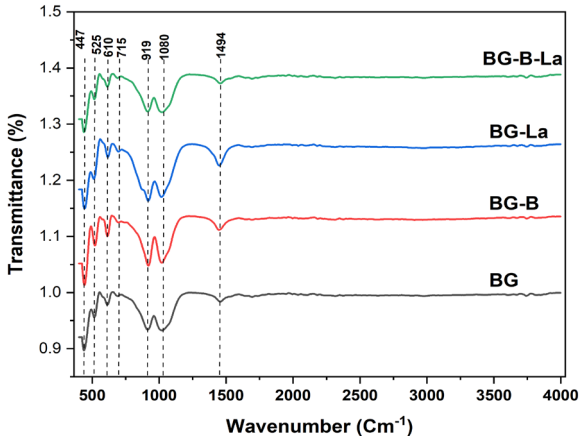

Fig. 5. FTIR for the samples before the immersion in SBF.

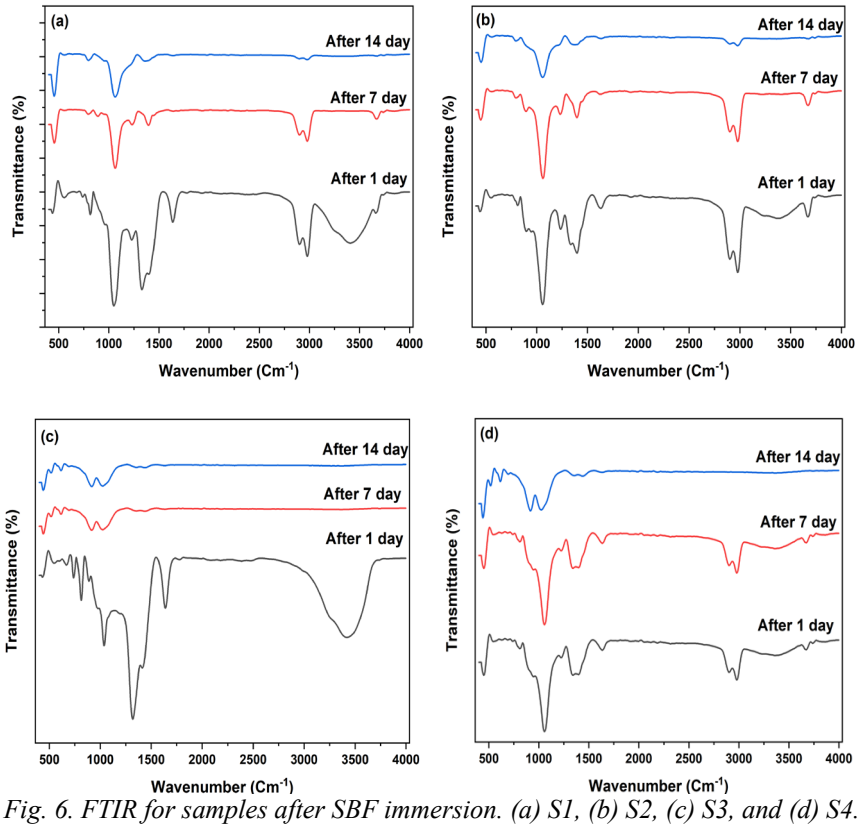

Fig. 6. FTIR for samples after SBF immersion. (a) S1, (b) S2, (c) S3, and (d) S4.

SEM analyses were performed on the surfaces of the prepared samples to examine the hydroxyapatite layer formed after immersion in artificial body fluid. The bioactive glass is shown in SEM images (Figures 7, 8) both before and after storage in SBF for 1 week and 14 days. After all samples were in SBF for 1, 7, and 14 days, a uniform white layer of hydroxyapatite was discovered covering their surfaces (Figure 8(a), (b), (c), and (d)). HA crystals were found to form in a filamentous structure, particularly in glass samples containing 5 wt.% B_2O_3 and 10 wt.% La_2O_3. However, it was found that the HA particles were randomly distributed and didn't cover the entire surface of the glass sample, which did not contain B_2O_3 or La_2O_3. The bioactive glass samples were subjected to EDS measurement simultaneously with the SEM analyses.

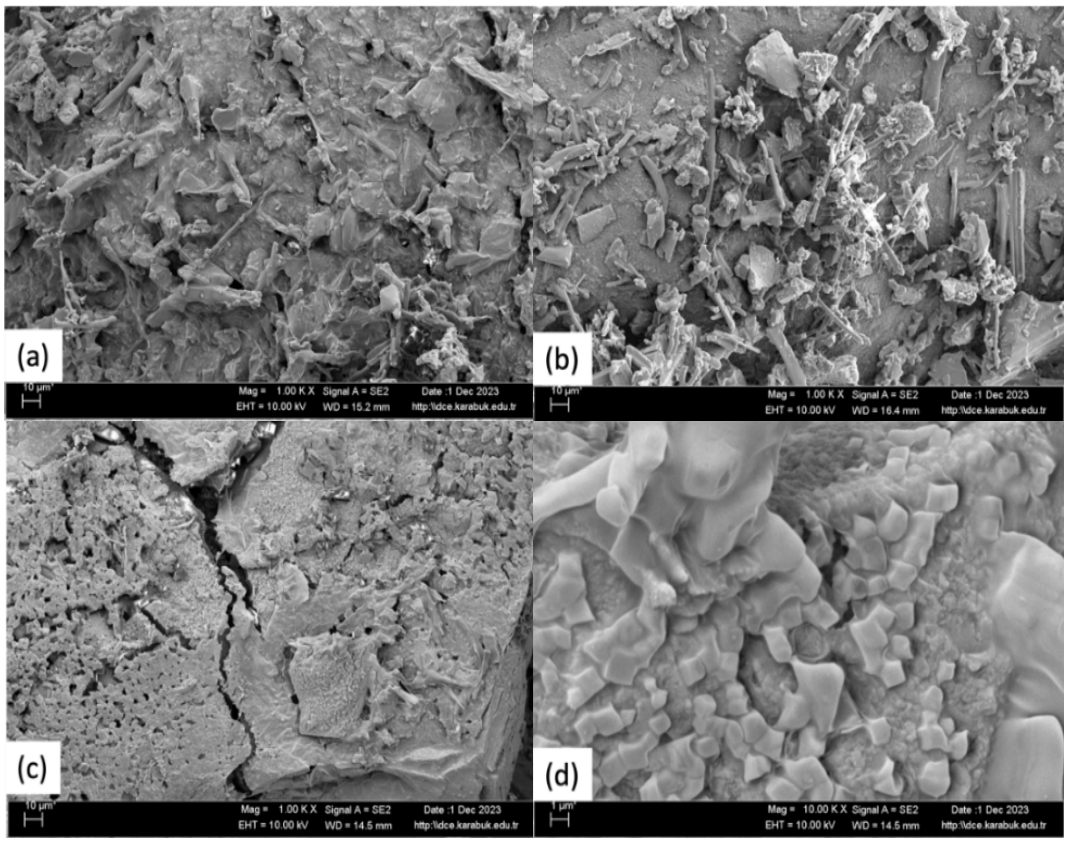

Fig. 7. SEM for the samples before the immersion in SBF.

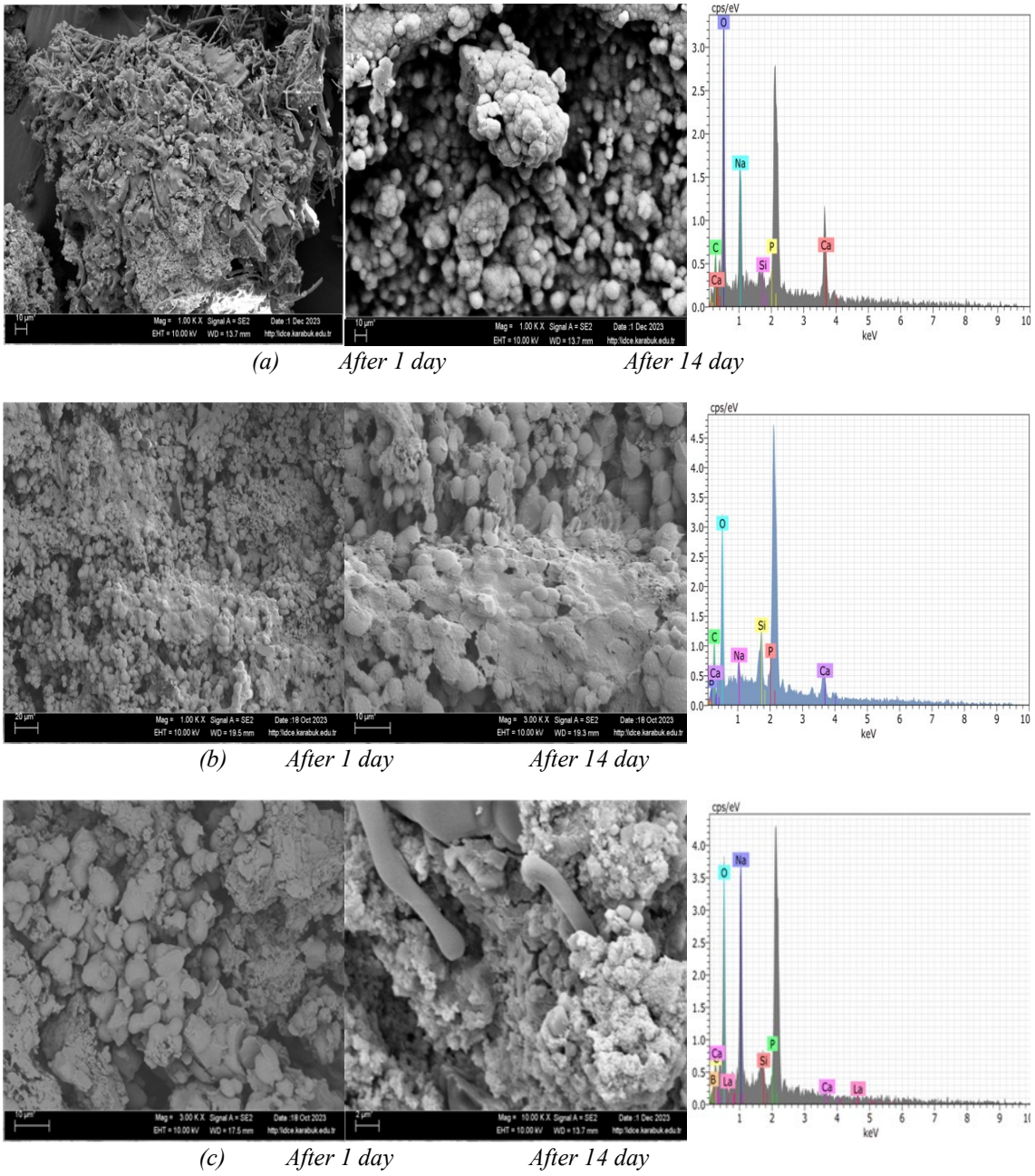

Fig. 8. SEM for samples after SBF immersion. (a) S1, (b) S2, (c) S3, and (d) S4.

An energy dispersive X-ray spectrograph (EDX) was used to analyze the elemental composition of glass samples immersed in simulated body fluid (SBF) for 14 days. The analysis confirmed the presence of the expected ions Si, Na, P, B, Ca and La. When the purity of the glass samples was examined, there was a small difference between their nominal and experimental composition, which was most likely due to elemental losses during the analytical melting process. The calculated Ca/P atomic ratio of the glass samples was approximately 1.67, which corresponded to the hydroxyapatite standard value. The results of the treated glass samples, which showed a significant correlation with the FTIR and XRD analyzes and showed the formation of an apatite layer.

All samples showed an increase in pH over time in Figure 9 due to ion exchange reactions releasing Na^{+}, Ca^{2+}, $B^{3+/4+}$, and La^{3+} ions that increased the OH^{-} concentration. The doped samples generally had higher pH values than the undoped glass, especially over longer periods of time. This suggests that the dissolution rate is increased due to network perturbations caused by the dopants.

La_2O_3 doping resulted in the highest pH value, followed by the combined B_2O_3+La_2O_3 doping. This indicates that La^{3+} is a more effective network modifier to improve degradation kinetics compared to $B^{3+/4+}$ .B_2O_3 doping also increased the pH, although to a lesser extent than La_2O_3, since $B^{3+/4+}$ is a less disruptive network former compared to the modifying behaviour of La^{3+}.The pH increase was more pronounced from days 1 to 7 than from days 7 to 14, with initial ion exchanges before equilibrium being reached having a greater impact. All results remained close to physiological pH and demonstrated that the materials maintain suitable conditions for osteointegration while doping alters their degradation profiles. Mesopores in these samples accelerate ion exchange due to their high reactivity and numerous pores, leading to an increase in pH because of the exchange.

Figure 10 b) shows the time course of weight loss when immersed in simulated body fluid (SBF) for the prepared samples. All samples experienced a gradual increase in weight loss as the SBF continued to degrade through hydration and ion exchange reactions. Doped samples showed higher weight loss compared to undoped glass, suggesting that the presence of dopants accelerated the dissolution process. Among the tested dopants, La_2O_3 caused the most significant weight loss, followed by the combination of B_2O_3+La_2O_3. This shows that La^{3+} has the most disruptive influence on the network structure. B_2O_3 doping also resulted in increased weight loss compared to the undoped sample, although lower than La_2O_3. The difference between the network modifying effects of La^{3+} and $B^{3+/4+}$ was evident in the weight loss results. Weight loss was more pronounced from days 1 to 7 than from days 7 to 14, suggesting faster resolution in the earlier days due to greater exchange. Despite the increasing weight loss, it remained below 15%, indicating that degradation was controlled, and soluble products were formed. The observed trends are consistent with pH changes and illustrate how different dopants can influence the dissolution rate of glass due to their network-modifying properties.

The stronger interaction between the SBF and the glass sample during the dissolution phase causes the bioactive glass-ceramic interface to be leached upon contact, Soaks water and forms an amorphous Ca/P layer [20] . Long-term incubation creates a crystallizing layer at the interface, which prevents surface erosion and promotes the development of a crystalline HA layer. Apatite, which is very similar to bone structure, is formed by the large pH fluctuations that lead to a loss of mass in the bioglasses. The occurrence of mineralization on the glass-ceramic surface is attributed to several factors, such as those that lead to a decrease in the sample mass and those that change the pH of the solution[21] . Materials derived from bioglass can transform into an apatite-like material when immersed in SBF. There has been much debate about the importance of this feature. According to their studies on the crystallization of glass ceramics, 45S5 bioglass, which was previously bioactive, changed to an inactive state upon crystallization an inactive state [22].

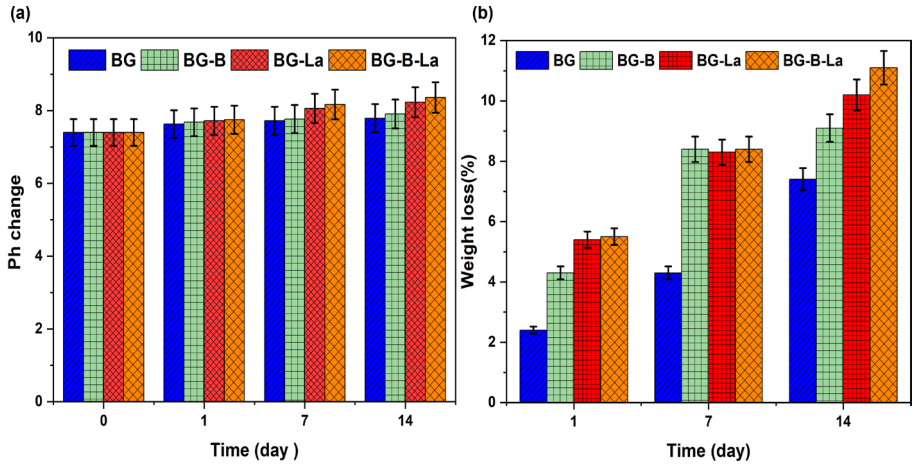

Fig. 9. Analysis of a) PH and b) weight loss of the glass-ceramic during SBF immersion.

The samples infused at 5% weight. 10% weight B_2O_3. La_2O_3 and five percent by weight in combination. Weight percent plus 10 wt.% B_2O_3 and La_2O_3 gave satisfactory results. Figure 10 illustrates the increase in density observed after adding these additives to the glass matrix. This improvement is explained by the fact that the introduced oxides had a higher density than the oxides they replaced. The results show that the density of B_2O_3, 2.46 g/cm3, is higher than that of Na_2O, and that of La_2O_3, 6.51 g/cm3, is higher than that of SiO_2, 2.65 g/cm3[23]. By adding 5 percent by weight, the mechanical properties of the samples could be significantly improved. B_2O_3, ten percent by weight La_2O_3 and a mixture of five percent by weight B_2O_3 and 10wt.% of La_2O_3. The improved compaction and reduced weak points are attributed to the increased density and reduced porosity of the glass ceramic material. The asymmetrical shape and uneven distribution of the pores, which act as sources of stress, are usually the cause of these weak points. The glass was transformed into a glass-ceramic material with significant crystallization through heat treatment, specifically sintering at 800 °C for three hours. Higher densification was achieved by a reduction in the distance between grains and some degree of partial melting that occurred as the sintering process approached the melting point of the samples. Due to the well-organized crystal structure, the mechanical strength is increased by preventing the propagation of cracks [24].

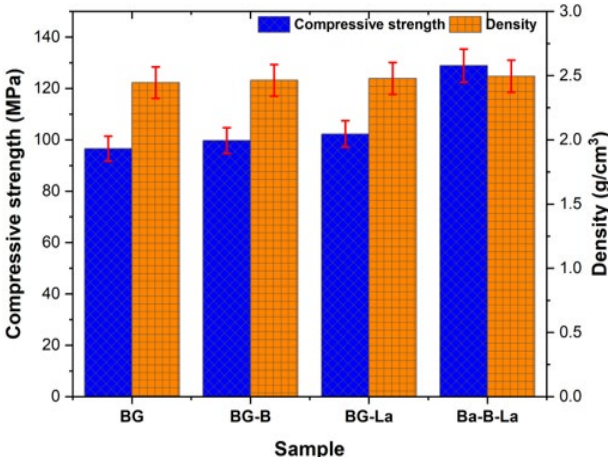

Fig. 10. Mechanical properties of the prepared samples.

In the antibacterial analysis, bioactive glass-ceramic samples with dimensions (H = 5 mm, D = 10 mm) were positioned on an agar plate containing common bacterial strains such as E. coli, S. aureus and S. epidermidis in vivo. These plates were then incubated at (37°C) and samples were taken after a period of 24 hours to assess bacterial activity. The presence of bacteria was indicated by the formation of a dark, circular halo around the samples, the diameter of which varied depending on bactericidal potency. All doped samples showed larger inhibition zones than the undoped BG, suggesting increased antibacterial activity of the dopants, as shown in Figure 11. BG-La and Ba-B-La had the largest zones, suggesting that doping with La_2O_3 promotes antibacterial properties more effectively than B_2O_3 alone , this could be because La_{3+} ions cause more damage to bacterial cell membranes than B_{3+}/B_{4+} at toxic threshold concentrations [25].

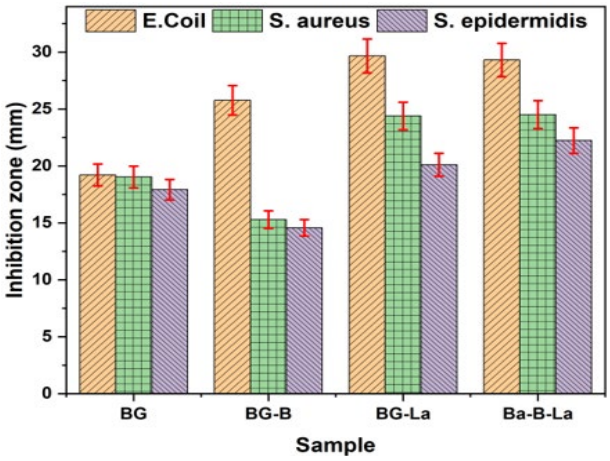

Fig. 11. Inhibition zone of the prepared samples against different types of bacteria.

4. Conclusion

45S5 with composition by weight; 45% SiO_2, 24.5% Na_2O, 6% P_2O_5 and 24.5% CaO) bioactive glasses, doped with boron and lanthanum oxides. The glass transition temperatures of 45S5 boron-lanthanum-doped bioactive glasses were 400–564 °C after applying DTA at a heating rate of 10 °C/min. XRD analysis identified the crystal phases formed in bioactive glass-ceramic samples as sodium calcium silicate ($Na_2Ca_2Si_3O_9$) and calcium silicate (Ca_2SiO_4). The samples soaked in body fluids developed a very thin layer of hydroxyapatite (HA) on their surface after being immersed in SBF for several days. The width of the XRD patterns was determined by the size of the crystals and the lattice strain; Larger peaks were produced by smaller or less ordered crystals. FTIR spectra confirmed the presence of a silicate network structure in the bioactive glass-ceramic, as expected given SiO_2 as the main component. Specific peaks were observed corresponding to the vibration modes of the PO_4^{-3}, Si-O-Si and BO groups within the material structure. Increasing La^{3+} ion concentration resulted in decreasing intensity of PO_4^{-3} peaks, suggesting that the structure and CaP binding geometry were changed by the presence of lanthanum. SEM images showed that the bioactive glass samples had an amorphous structure before immersing in SBF. After 1, 7, and 14 days of soaking, the surfaces were uniformly covered with a layer of hydroxyapatite (HA), with white HA crystals seen in a filamentous structure, especially in glasses containing 5% B_2O_3 and 10% La_2O_3. EDS point analysis measurements detected calcium and phosphorus on sample surfaces, confirming HA deposition. All samples showed an increase in pH over time due to ion exchange reactions releasing Na^+, Ca^{2+}, $B^{3+/4+}$ and La^{3+} ions, which increase the OH^- concentration. Doped samples generally had higher pH values than undoped glass, especially at longer times. La_2O_3 and combined B_2O_3+La_2O_3 doping are most effective in accelerating material degradation kinetics and mass loss profiles by increasing network connectivity disruption. Doping with B_2O_3 and La_2O_3 along with sintering heat treatment produced a densified glass-ceramic microstructure with improved mechanical properties through reduced porosity, ordered crystallization, and crack growth inhibition compared to the original glass shape. Composition and processing optimizations validated through physical characterization improved the material. Doping with B_2O_3 and La_2O_3 improves the inhibitory properties compared to undoped BG, with La_2O_3 producing the strongest effects overall. Optimal antibacterial functionality can be achieved through combinatorial doping.

Acknowledgments

This work was supported by the Scientific Research Projects Coordination Unit of Karabuk University. Project number: KBÜBAP-23-YL-122.

References

[1] Al-Murshdy JMS, Al-Deen HHJ, Hussein SR, Journal of Bio-and Tribo-Corrosion. 2021;7:1-18; https://doi.org/10.1007/s40735-021-00581-w

[2] Majdi HS, Saud A, Al-Mamoori M., A Novel Nanocomposite (SR/HA/-nZnO) Material for Medical Application. Springer; 2020:333-341; https://doi.org/10.1007/978-3-030-31866-6_63

[3] Al-Humairi ANS, Majdi HS, Al-Humairi SNS, Al-Maamori M., Biomaterials: Multidisciplinary approaches and their related applications. White Falcon Publishing; 2020.

[4] Okay E, Ozarslan AC, Başal Ö, et al., Cureus. 2023;15(7); https://doi.org/10.7759/cureus.41521

[5] Pan H, Zhao X, Zhang X, et al., Journal of the Royal Society Interface. 2010;7(48):1025-1031; https://doi.org/10.1098/rsif.2009.0504

[6] Ben-Arfa BA, Pullar RC., Processes. 2020;8(5):615; https://doi.org/10.3390/pr8050615

[7] Yilmaz B, Pazarceviren AE, Tezcaner A, Evis Z., Microchemical Journal. 2020;155:104713; https://doi.org/10.1016/j.microc.2020.104713

[8] Hesaraki S, Alizadeh M, Nazarian H, Sharifi D., Journal of Materials Science: Materials in Medicine. 2010;21:695-705; https://doi.org/10.1007/s10856-009-3920-0

[9] Saud AN, Koç E, Özdemir O., Ceramics International. 2022; https://doi.org/10.1016/j.ceramint.2022.11.093

[10] Lee E-J, Kim H-W, Knowles JC., Stem Cell Biology and Tissue Engineering in Dental Sciences. Elsevier; 2015:163-174; https://doi.org/10.1016/B978-0-12-397157-9.00014-X

[11] Hench LL, Ethridge E. Biomaterials: an interfacial approach. (No Title). 1982;

[12] Davies JE. Bone-Bio Material Interface. University of Toronto Press; 1991; https://doi.org/10.3138/9781442671508

[13] Hossein Jodati BG, Zafer Evis, Dilek Keskin , Ayşen Tezcaner, Ceramics International. 2020;46(8)(A):10503-10511; https://doi.org/10.1016/j.ceramint.2020.01.050

[14] Awais Ali Aslam JA, Rana Adeel Mehmood, Arifa Mubarak, Amna Khatoon, Uzma Akbar, Sheikh Asrar Ahmad, Muhammad Atif, Ceramics International. 2023;49(12):19595-19605; https://doi.org/10.1016/j.ceramint.2023.03.164

[15] Saud AN, Koç E, Özdemir O., Ceramics International. 2023; https://doi.org/10.1016/j.ceramint.2023.06.002

[16] Chitra S, Bargavi P, Durgalakshmi D, Rajashree P, Balakumar S., Processing and Application of Ceramics. 2019;13(1):12-23; https://doi.org/10.2298/PAC1901012C

[17] Singh RK, Kothiyal G, Srinivasan A., Arch Bioceram Res. 2008;8:89-92; https://doi.org/10.1016/j.apsusc.2009.02.089

[18] Nayak J, Kumar S, Bera J, Journal of Non-Crystalline Solids. 2010;356(28-30):1447-1451; https://doi.org/10.1016/j.jnoncrysol.2010.04.041

[19] Filho OP, La Torre GP, Hench LL. Journal of Biomedical Materials Research: An Official Journal of The Society for Biomaterials and The Japanese Society for Biomaterials. 1996;30(4):509-514; https://doi.org/10.1002/(SICI)1097-4636(199604)30:4<509::AID-JBM9>3.0.CO;2-T

[20] Kaou MH, Furkó M, Balázsi K, Balázsi C., Nanomaterials. 2023;13(16):2287; https://doi.org/10.3390/nano13162287

[21] Aneb K, Oudadesse H, Khireddine H, Lefeuvre B, Lucas A., Journal of Sol-Gel Science and Technology. 2024;109(2):502-522; https://doi.org/10.1007/s10971-023-06290-9

[22] Huang G, Liu S-Y, Wu J-L, Qiu D, Dong Y-M., Journal of Dental Sciences. 2022;17(1):217-224; https://doi.org/10.1016/j.jds.2021.04.018

[23] Thomas H, Ghosh M, Dey KK, Gautam C., Phys Scr. 2023;98:105918; https://doi.org/10.1088/1402-4896/acf539

[24] Zhang Y, Zhu B, Cai X, et al., Colloids and Surfaces A: Physicochemical and Engineering Aspects. 2023;674:131874; https://doi.org/10.1016/j.colsurfa.2023.131874
[25] Peng L, Yi L, Zhexue L, et al., Journal of inorganic biochemistry. 2004;98(1):68-72; https://doi.org/10.1016/j.jinorgbio.2003.08.012